

DISCOVERY OF THE BROAD-LINED TYPE Ic SN 2013cq ASSOCIATED WITH THE VERY ENERGETIC GRB 130427A

D. XU¹, A. DE UGARTE POSTIGO^{2,1}, G. LELOUDAS^{3,1}, T. KRÜHLER¹, Z. CANO⁴, J. HJORTH¹, D. MALESANI¹, J. P. U. FYNBO¹, C. C. THÖNE², R. SÁNCHEZ-RAMÍREZ², S. SCHULZE^{5,6}, P. JAKOBSSON⁴, L. KAPER⁷, J. SOLLERMAN⁸, D. J. WATSON¹, A. CABRERA-LAVERS⁹, C. CAO^{10,19}, S. COVINO¹¹, H. FLORES¹², S. GEIER^{1,13}, J. GOROSABEL^{2,14,15}, S. M. HU¹⁰, B. MILVANG-JENSEN¹, M. SPARRE¹, L. P. XIN¹⁶, T. M. ZHANG¹⁶, W. K. ZHENG¹⁷, AND Y. C. ZOU¹⁸

¹ Dark Cosmology Centre, Niels Bohr Institute, University of Copenhagen, Juliane Maries Vej 30, DK-2100 København Ø, Denmark; dong@dark-cosmology.dk

² Instituto de Astrofísica de Andalucía, CSIC, Glorieta de la Astronomía s/n, E-18008 Granada, Spain

³ The Oskar Klein Centre, Department of Physics, Stockholm University, AlbaNova, SE-10691 Stockholm, Sweden

⁴ Centre for Astrophysics and Cosmology, Science Institute, University of Iceland, Dunhagi 5, IS-107 Reykjavík, Iceland

⁵ Departamento de Astronomía y Astrofísica, Pontificia Universidad Católica de Chile, Casilla 306, Santiago 22, Chile

⁶ Millennium Center for Supernova Science, Chile

⁷ Astronomical Institute Anton Pannekoek, University of Amsterdam, Science Park 904, NL-1098 XH Amsterdam, The Netherlands

⁸ The Oskar Klein Centre, Department of Astronomy, Stockholm University, AlbaNova, SE-10691 Stockholm, Sweden

⁹ Instituto de Astrofísica de Canarias, E-38205 La Laguna, Tenerife, Spain

¹⁰ Department of Space Science and Physics, Shandong University at Weihai, Weihai, Shandong 264209, China

¹¹ INAF/Brera Astronomical Observatory, via Bianchi 46, I-23807 Merate (LC), Italy

¹² Laboratoire Galaxies Etoiles Physique et Instrumentation, Observatoire de Paris, 5 place Jules Janssen, F-92195 Meudon, France

¹³ Nordic Optical Telescope, Apartado 474, E-38700 Santa Cruz de La Palma, Spain

¹⁴ Unidad Asociada Grupo Ciencia Planetarias UPV/EHU-IAA/CSIC, Departamento de Física Aplicada I, E.T.S. Ingeniería,

Universidad del País Vasco UPV/EHU, Alameda de Urquijo s/n, E-48013, Bilbao, Spain

¹⁵ Ikerbasque, Basque Foundation for Science, Alameda de Urquijo 36-5, E-48008 Bilbao, Spain

¹⁶ National Astronomical Observatories, Chinese Academy of Sciences, Beijing 100012, China

¹⁷ Department of Astronomy, University of California, Berkeley, CA 94720-3411, USA

¹⁸ School of Physics, Huazhong University of Science and Technology, Wuhan 430074, China

Received 2013 May 30; accepted 2013 August 19; published 2013 October 3

ABSTRACT

Long-duration gamma-ray bursts (GRBs) at $z < 1$ are found in most cases to be accompanied by bright, broad-lined Type Ic supernovae (SNe Ic-BL). The highest-energy GRBs are mostly located at higher redshifts, where the associated SNe are hard to detect observationally. Here, we present early and late observations of the optical counterpart of the very energetic GRB 130427A. Despite its moderate redshift, $z = 0.3399 \pm 0.0002$, GRB 130427A is at the high end of the GRB energy distribution, with an isotropic-equivalent energy release of $E_{\text{iso}} \sim 9.6 \times 10^{53}$ erg, more than an order of magnitude more energetic than other GRBs with spectroscopically confirmed SNe. In our dense photometric monitoring, we detect excess flux in the host-subtracted r -band light curve, consistent with that expected from an emerging SN, ~ 0.2 mag fainter than the prototypical SN 1998bw. A spectrum obtained around the time of the SN peak (16.7 days after the GRB) reveals broad undulations typical of SNe Ic-BL, confirming the presence of an SN, designated SN 2013cq. The spectral shape and early peak time are similar to those of the high-expansion velocity SN 2010bh associated with GRB 100316D. Our findings demonstrate that high-energy, long-duration GRBs, commonly detected at high redshift, can also be associated with SNe Ic-BL, pointing to a common progenitor mechanism.

Key words: gamma-ray burst: individual (GRB 130427A) – supernovae: individual (SN 2013cq)

Online-only material: color figures

1. INTRODUCTION

The standard paradigm for long-duration gamma-ray bursts (GRBs) involves a broad-lined Type Ic supernova (SN Ic-BL) with $M_V \sim -19$ mag (Woosley & Bloom 2006; Hjorth & Bloom 2012), such as those predicted by the collapsar model (MacFadyen & Woosley 1999). This fact is based on spectroscopic evidence in SNe from low-luminosity GRBs (Bromberg et al. 2011) such as SN 1998bw accompanying GRB 980425 (Galama et al. 1998), as well as relatively higher-luminosity GRBs, such as SN 2003dh accompanying GRB 030329 (Hjorth et al. 2003; Stanek et al. 2003). Interestingly, for the two low-redshift cases of GRB 060505 and GRB 060614, no associated SN was found to deep limits (Fynbo et al. 2006; Della Valle

et al. 2006; Gal-Yam et al. 2006), but since then no similar events have been reported.

GRB 130427A (Maselli et al. 2013; Elenin et al. 2013) is remarkable as it is both extremely energetic and located at a moderately low redshift of $z = 0.3399 \pm 0.0002$ (Levan et al. 2013 and this work). Using the spectral parameters for the prompt emission given by von Kienlin (2013), we derive an isotropic gamma-ray energy²⁰ of $E_{\text{iso}} = (9.61 \pm 0.04) \times 10^{53}$ erg in the 1–10000 keV rest-frame energy band. The optical afterglow peaked at $R \approx 7.4$ mag during the prompt emission phase (Wren et al. 2013). Only $\sim 5\%$ of all GRBs with measured redshifts are at such a small distance (see, e.g., Jakobsson et al. 2012; Figure 1) and those are usually low-luminosity events. In contrast, GRB 130427A was an extremely energetic burst and

¹⁹ Visiting Scholar, Infrared Processing and Analysis Center, Caltech, Pasadena, CA 91125, USA.

²⁰ We adopt a Λ CDM cosmology with $H_0 = 67.3 \text{ km s}^{-1} \text{ Mpc}^{-1}$, $\Omega_m = 0.315$, and $\Omega_\Lambda = 0.685$ (Planck Collaboration 2013).

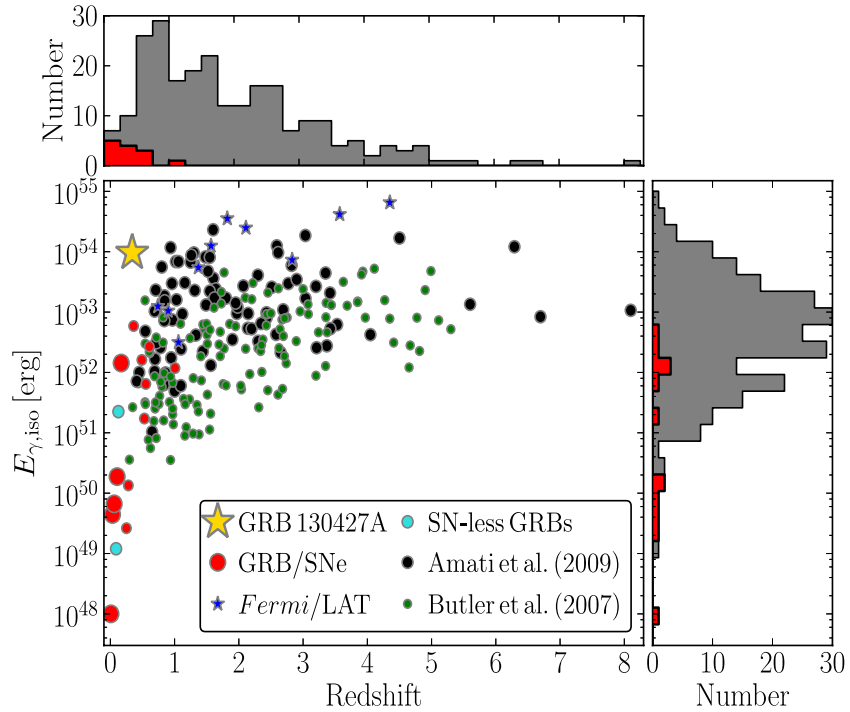


Figure 1. Isotropic-equivalent energy release in gamma-rays E_{iso} of GRB 130427A compared with different GRB samples. GRB/SN associations classified with rank A (larger circles) or B (smaller circles) in Hjorth & Bloom (2012) are plotted in red and nearby GRBs without a luminous SN are shown as light blue circles (Fynbo et al. 2006). We show GRBs detected by *Fermi*/LAT (McBreen et al. 2010; Fermi-LAT Collaboration 2013) as blue stars, GRBs from Amati et al. (2009) as black circles, and *Swift* GRBs derived by Butler et al. (2007) as green circles. For GRBs appearing in several of the aforementioned catalogs, earlier referenced data take preference over later ones. Due to various reasons such as instrumental constraints, GRB coordinates, weather coordinations, and so on, a substantial fraction of GRBs at $z < 1$ were not able to be effectively checked whether they were associated with SNe, although they are believed to be with SNe based on those SN-associated GRBs at $z < 1$.

(A color version of this figure is available in the online journal.)

hence it has enabled detailed studies of a system analogous to those usually only found at higher redshifts (Fan et al. 2013; Laskar et al. 2013; Tam et al. 2013).

Due to the dearth of such extremely luminous GRBs at low redshift and their faintness at high redshift, we so far have had no spectroscopic evidence for accompanying SNe in very energetic GRBs with $E_{\text{iso}} > 10^{52.7}$ erg (for photometric evidence of an SN associated with the very energetic GRB 080319B, see Tanvir et al. 2010). In Figure 1, we show the gamma-ray energy release of GRBs as a function of redshift. Overplotted are systems with spectroscopic evidence for an SN. GRB 130427A stands out as an exceptional system. It is unclear if progenitor models involving an SN can power such energetic GRBs (see, e.g., Piran 2004). Observationally, it has proven to be difficult to test the SN properties of these events. In this work, we focus on the search for and discovery of an SN accompanying this remarkable burst.

2. OBSERVATIONS AND DATA ANALYSIS

2.1. Photometry

Our first follow-up photometry was carried out at the 1 m optical telescope located in Weihai, Shandong Province, China. The bright optical counterpart of the GRB was well detected in the Cousins R_C filter at $R_C \sim 15.5$ mag 4.178 hr after the burst. Initially, the Sloan Digital Sky Survey (SDSS) filters were not available at the telescope, but two days into our monitoring campaign, SDSS r and i filters were installed and have been available since then.

Our photometric follow-up observations were mainly obtained at the 2.5 m Nordic Optical Telescope (NOT) using the

ALFOSC instrument. Photometry was primarily obtained in the r band, complemented by $ugiz$ data useful for monitoring the spectral evolution of the counterpart. As shown in Figure 2, there is indication from the NOT images that the GRB counterpart lies in the northwest part of an extended host galaxy. With our spatial resolution, the afterglow is blended with the host and we thus use a relatively large aperture ($\approx 3.8''$ in diameter) to measure the magnitudes of the counterpart plus host. Using a smaller aperture would provide lower fluxes, but the host contribution would be hard to quantify, especially at late times (i.e., ~ 10 days and beyond after the burst). In this way, we consistently include most of the host light.

Additionally, follow-up observations were obtained at the 2.16 m telescope in Xinglong, Hebei Province, China. Photometry was obtained in the Cousins R_C and I_C filters and then transformed to SDSS r and i magnitudes based on our afterglow spectra.

All optical data were reduced in a standard way using IRAF v2.15 in the Scisoft 7.7 package. Magnitudes were calibrated with two nearby bright SDSS field stars, SDSS J113230.55+274420.3 and SDSS J113220.11+274133.5,²¹ whose zero-point errors were 0.01 mag and were propagated into the final magnitude measurements. The SDSS r -band light curve is presented in Figure 3 and a log of the observations is shown in Table 1.

We fit the NOT multi-color photometry taken in the first night after the trigger ($g = 17.31 \pm 0.01$ mag, $r = 17.06 \pm 0.01$ mag,

²¹ <http://skyserver.sdss3.org/public/en/tools/chart/navi.aspx?ra=173.1362&dec=27.7129&opt=I>

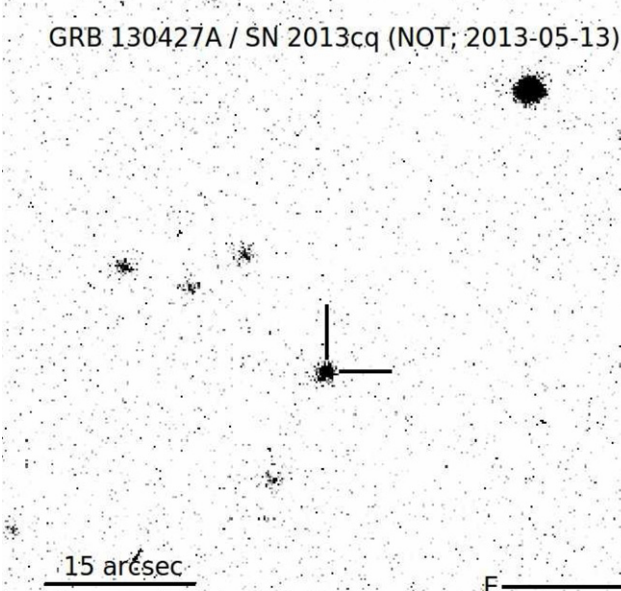


Figure 2. Field of GRB 130427A/SN 2013cq taken at the NOT/ALFOSC at 00:18 UT on 2013 May 13, when it was close to the GTC spectrum time of 00:35 UT on 2013 May 14. North is up and east is to the left. The angular resolution is $0''.19 \text{ pixel}^{-1}$ and it is clear that the GRB/SN lies in the northwest part of its extended host galaxy.

$i = 16.92 \pm 0.01 \text{ mag}$, $z = 16.86 \pm 0.02 \text{ mag}$) and the simultaneous X-ray spectrum by the X-ray Telescope (XRT) on board the *Swift* mission.²² Using synchrotron models and extinction laws from the Local Group (see Krühler et al. 2011 for details), we estimate the reddening of the host to be $E(B - V)_{\text{host}} = 0.05 \pm 0.02 \text{ mag}$ for a Milky Way-type

²² http://www.swift.ac.uk/xrt_curves/554620

extinction law. Within the errors, this value is consistent with the reddening derived assuming an SMC or LMC extinction law because of the small amount of reddening and the wavelength range probed by our observations.

2.2. Spectroscopy

Our first spectrum was obtained using NOT/ALFOSC. The total exposure was 1800 s with a mean time of 0.44 days post-burst. The spectrum covers the range 3200–9100 Å with a resolving power of ~ 700 . We identify prominent absorption lines of Mg II 2796 & 2803, Mg I 2852, and Ca II 3934 & 3968, as well as weak emission lines of [O II] 3727 and H β , all at a common redshift of $z = 0.34$.

A second spectrum with intermediate resolution was obtained shortly afterward using the Very Large Telescope (VLT) equipped with the XSHOOTER spectrograph. The continuum was well detected over the full range 3000–24800 Å. A number of absorption features are visible, including Fe II 2344, Mn II 2577, Mg II 2796 & 2803, Mg I 2852, Ti II 3074, Ca II 3934 & 3968, Na I 5890 & 5896, and emission lines such as [O II] 3727, H β , [O III] 5007, and H α , all at a common redshift of $z = 0.3399 \pm 0.0002$. In the XSHOOTER spectrum, Na I D 5890 & 5896 absorption was detected at the redshift of the host. We measure equivalent widths of 0.18 ± 0.02 and $0.08 \pm 0.03 \text{ Å}$ for the Na I D1 and D2 components, respectively. Using the relations in Poznanski et al. (2012), we obtain an estimate for $E(B - V)_{\text{host}} = 0.03 \pm 0.01 \text{ mag}$, but remark that there exists a substantial dispersion of $E(B - V) \sim 0.15 \text{ mag}$ in this relation. Considering different calibrations/systematics involved in the above $E(B - V)_{\text{host}}$ measurements, we adopt $E(B - V)_{\text{host}} = 0.05 \text{ mag}$ for the host extinction.

Given the relatively low redshift, we planned a third spectroscopic observation with the aim of detecting SN signatures. Based on the light curve evolution, we obtained a spectrum of the optical counterpart and host galaxy with the 10.4 m Gran

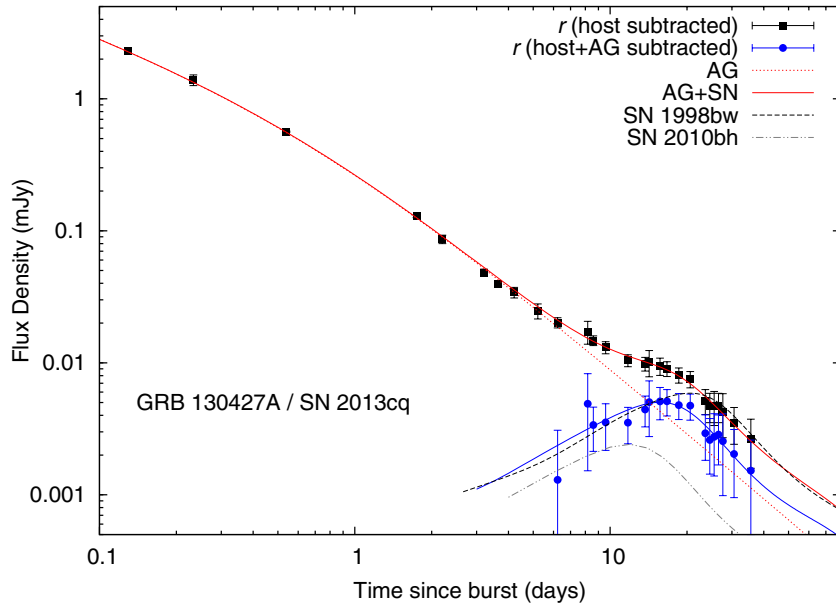


Figure 3. SDSS r -band light curve of GRB 130427A/SN 2013cq in the observer frame. Filled squares denote host-subtracted magnitudes, while filled circles are host- and afterglow- (AG) subtracted magnitudes. The shape and brightness of the latter are consistent with that of a core-collapse supernova. The red dashed line is our AG model (see the text for the best-fitting parameters). The blue solid line plotted against the light curve of SN 2013cq is a model supernova. SN 2013cq peaks earlier than SN 1998bw and is about 0.2 mag fainter in the rest-frame B band.

(A color version of this figure is available in the online journal.)

Table 1
Log of the SDSS *r*-band Observations and Photometry

Mid Time ^a (days)	Mag ^b	Error	Instrument
0.538	17.06	0.02	NOT/ALFOSC
1.745	18.59	0.02	NOT/ALFOSC
2.204	18.98	0.07	WH/PI
3.205	19.51	0.05	WH/PI
3.648	19.68	0.02	NOT/ALFOSC
4.21	19.80	0.07	WH/PI
5.21	20.05	0.09	WH/PI
6.23	20.19	0.05	XL/BFOSC
8.17	20.30	0.12	WH/PI
8.60	20.39	0.03	NOT/ALFOSC
9.60	20.46	0.04	NOT/ALFOSC
11.74	20.58	0.02	NOT/ALFOSC
13.71	20.61	0.03	NOT/ALFOSC
14.22	20.60	0.10	XL/BFOSC
15.69	20.63	0.05	NOT/ALFOSC
16.70	20.65	0.03	GTC/OSIRIS
18.59	20.70	0.02	NOT/ALFOSC
20.59	20.73	0.02	NOT/ALFOSC
23.61	20.87	0.03	NOT/ALFOSC
24.57	20.90	0.04	NOT/ALFOSC
25.56	20.90	0.06	NOT/ALFOSC
26.57	20.90	0.04	NOT/ALFOSC
27.64	20.93	0.08	NOT/ALFOSC
30.58	20.98	0.03	NOT/ALFOSC
35.57	21.04	0.03	NOT/ALFOSC

Notes.

^a The middle time of each epoch, in units of days post-burst, relative to the *Fermi* trigger time of 07:47:06 UT on 2013 April 27, ~ 51 s ahead of the *Swift* trigger time of this burst.

^b Magnitudes not corrected for a Galactic reddening of $E(B - V)_{\text{MW}} = 0.02$ mag.

Telescopio Canarias (GTC) 16.7 days after the GRB. This time corresponds to 12.5 days in the GRB rest frame. Observations were 4×1200 s, covering the range of 4800–10000 Å with a resolving power of ~ 600 . The slit was oriented to cover both the afterglow position and the host galaxy nucleus.

All spectroscopic data were reduced in a standard way using dedicated IRAF pipelines or European Southern Observatory (ESO) pipelines. The resulting spectra are presented in Figure 4.

2.3. Host Galaxy

We use the catalogued pre-explosion imaging from the SDSS “DRS” (Aihara et al. 2011) to estimate physical properties of the GRB host galaxy and build a physical model of the stellar emission. The SDSS *ugriz* photometry was fitted within the LePhare program (Arnouts et al. 1999; Ilbert et al. 2006) using stellar population synthesis models from Bruzual & Charlot (2003), as detailed in Krühler et al. (2011). Based on the model fit to the data (Figure 4), we derive a luminosity $M_B = -19.8 \pm 0.2$ mag, a stellar mass of $M_\star = 10^{9.0 \pm 0.2} M_\odot$, a star-formation rate $\text{SFR}_{\text{SED}} = 2_{-1}^{+5} M_\odot \text{ yr}^{-1}$, and an age of the starburst $\tau = 400_{-250}^{+560}$ Myr for the host of GRB 130427A.

Host galaxy emission lines are detected above the SN continuum, including [N II] 6584 in the GTC spectrum, albeit at low significance. These detections allow us to place constraints on the metallicity of the explosion host environment using the calibrations in Pettini & Pagel (2004). We measure $\text{log(O/H)} + 12 = 8.43 \pm 0.07$ and 8.51 ± 0.09 using the O3N2

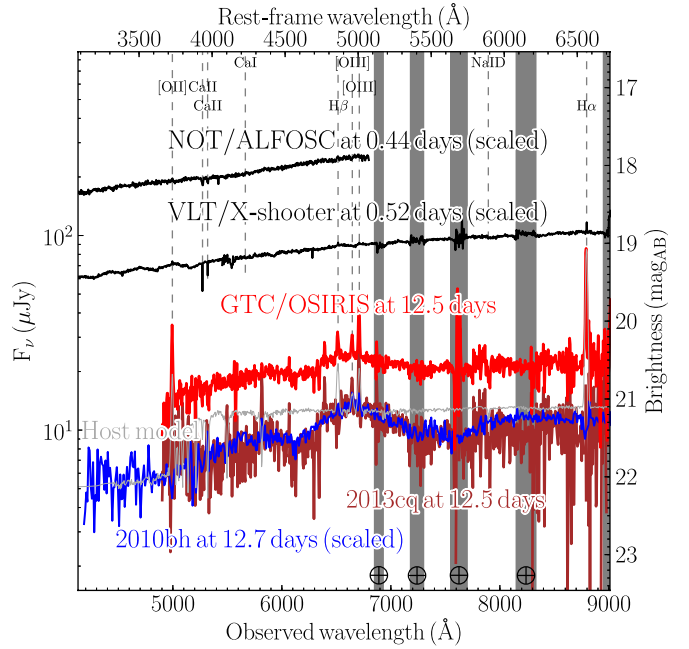


Figure 4. Spectroscopic sequence of GRB 130427A/SN 2013cq. Epochs of the spectra in their rest frames are marked, together with prominent emission and absorption lines and telluric bands (circled crosses as well as gray shaded areas). The top two (black) spectra were obtained from NOT/ALFOSC and VLT/XSHOOTER during the burst night. The red part of the NOT spectrum is affected by fringing (in gray). The original GTC, the host galaxy, and the host-subtracted GTC spectra are shown in red, gray, and wine, respectively. The host-subtracted spectrum is well matched by the broad-lined Type Ic SN 2010bh 12.7 days post-burst, very close to the 12.5 days of SN 2013cq here. (A color version of this figure is available in the online journal.)

and the N2 methods, respectively (statistical errors only), which is at the top right of the GRB-SN range in the metallicity– $M_{B,\text{host}}$ plane, similar to the cases of SNe Ic-BL without observed GRBs and SNe Ib+IIL (see Figure 2 in Modjaz et al. 2011). We note that the host galaxy also nicely lies within the 1σ dispersion of the mass–metallicity relation for normal field galaxies (Kewley & Ellison 2008). After including the systematic dispersion of 0.14 and 0.18 dex (Pettini & Pagel 2004) for the two methods, respectively, these results translate to a metallicity of 0.55 ± 0.19 and $0.67 \pm 0.25 Z_\odot$, respectively (Asplund et al. 2009).

3. SN 2013cq ASSOCIATED WITH GRB 130427A

3.1. Decomposition of the GTC Spectrum

We scaled the GTC spectrum by our simultaneous photometry from the same night, dereddened it by $E(B - V)_{\text{MW}} = 0.02$ mag (Schlegel et al. 1998), where the subscript refers to the Milky Way galaxy, brought it to the same resolution, and then subtracted the model host galaxy spectrum. These steps resulted in a “clean” spectrum of the transient. Afterward, the spectrum was dereddened by $E(B - V)_{\text{host}} = 0.05$ mag for the host extinction at $z = 0.34$. Both the original and the final GTC spectra are shown in Figure 4.

Although the resulting spectrum is noisy, it shows clear SN features, with the most prominent being a strong bump peaking at ~ 6700 Å (observer-frame; ~ 5000 Å rest-frame). The features are broad (and no H or He can be seen), justifying the classification of SN 2013cq as an SN Ic-BL (de Ugarte Postigo et al. 2013).

SN 1998bw (Patat et al. 2001), associated with GRB 980425, does not provide a good spectral match to SN 2013cq, mainly

because its main peak is located more to the red (rest-frame $\sim 5200 \text{ \AA}$ at similar phases). The same is true for SN 2006aj (Pian et al. 2006; Sollerman et al. 2006), associated with GRB 060218. Instead, we find a better match with SN 2010bh, associated with GRB 100316D, which is known to have high expansion velocities, up to $10,000 \text{ km s}^{-1}$ higher than other previous SNe Ic-BL associated with GRBs at all phases (Bufano et al. 2012). In particular, the best match is obtained with the spectrum of SN 2010bh at a rest-frame time of 12.7 days, very close to the rest-frame time of 12.5 days for SN 2013cq here (shown in Figure 4). The similarity with SN 2010bh is striking although there may be small color differences (e.g., the difference redward of $\sim 7500 \text{ \AA}$), which may reflect the diversity in GRB-SN spectra and/or the uncertain extinction correction toward SN 2010bh. Considering that the P-Cygni feature on the left of the strong bump can be primarily attributed to Fe II 5169, we measure an expansion velocity of $v_{\text{ph}} \sim 32,000 \text{ km s}^{-1}$ from the absorption minimum. This velocity is very similar to the peak photospheric velocity of SN 2010bh, $v_{\text{peak}} \sim 35,000 \text{ km s}^{-1}$ (Bufano et al. 2012).

3.2. Decomposition of the r-band Light Curve

The r-band light curve presented in Figure 3 has been corrected for foreground extinction ($E(B-V)_{\text{MW}} = 0.02 \text{ mag}$). From the foreground extinction-corrected flux, we subtract the contribution of the host galaxy ($r_{\text{host}} = 21.26 \pm 0.09$, as determined via photometry of pre-explosion SDSS imaging), so that the flux powering the light curve can be attributed solely to the afterglow and the accompanying SN. Visual inspection of the light curve reveals a deviation away from a power-law decay a few days post-burst, followed by a plateau that lasts for about 10 days, before decaying further. At the time the GTC spectrum was obtained, the Galactic extinction-corrected flux of the SN/afterglow was 1.85 times that of the host galaxy.

Next, we fit a smoothly broken power-law model (Beuermann et al. 1999) to the light curve up to the first four days (some r-band data points < 3 days published in the Gamma-ray Coordinates Network (GNC) circulars are used for the fitting; Perley & Cenko 2013; Wiggins 2013; Butler et al. 2013; Zhao et al. 2013) and derive the following best-fit parameters: $\alpha_1 = 0.69 \pm 0.13$, $\alpha_2 = 1.66 \pm 0.18$, and $t_{\text{break}} = 0.62 \pm 0.48$ days (the smoothness factor of the break is fixed to be unity and $\chi^2/\text{dof} = 1.47$ for 7 degrees of freedom, dof). This afterglow model is then subtracted from the already host-subtracted light curve and the resultant flux resembles that of an SN both in brightness and shape (e.g., Cano et al. 2011a). The peak brightness of SN 2013cq is found to be $r = 22.13 \text{ mag}$ at ~ 15.2 days observer-frame (~ 11.3 days rest-frame). At $z = 0.34$, the observer-frame r band corresponds approximately to the rest-frame B band, and we find that SN 2013cq has an absolute B-band magnitude of $M_B = -18.97 \pm 0.14$, which is about 0.2 mag fainter than SN 1998bw.

We then compare the optical properties of SN 2013cq with two other GRB-associated SNe: SN 1998bw and SN 2010bh. We create synthetic r-band light curves of SN 1998bw and SN 2010bh as they would appear at $z = 0.34$. Next, using Equations 1 and 2 from Cano et al. (2011b), we determine the stretch (s) and luminosity factor (k) of SN 2013cq relative to SN 1998bw: $s = 0.77 \pm 0.03$ and $k = 0.85 \pm 0.03$.

We further estimate the bolometric properties of SN 2013cq. The method, developed by Cano (2013), uses the relative stretch and luminosity factors of an SN relative to a template (in this case, SN 1998bw) and makes the assumption that the relative

shape of a given SN in a given filter is a good proxy for the relative shape of the SN bolometric light curve relative to the template. The bolometric light curve of the template²³ is then altered by s and k and then fit with an analytical model derived from Arnett (1982). The Arnett model depends on knowing the photospheric velocity at peak bolometric light to determine the ejecta mass and explosion energy, which for many SNe is determined from the velocity of different species in the SN spectra at peak light. We have used the photospheric velocity value determined in Section 3.1 (i.e., $v_{\text{ph}} \sim 32,000 \text{ km s}^{-1}$). In comparison with SN 1998bw, for SN 2013cq (in UBVRIJH), we derived its Ni mass, ejecta mass, and kinetic energy to be $M_{\text{Ni}} = 0.28 \pm 0.02 M_{\odot}$, $M_{\text{ej}} = 6.27 \pm 0.69 M_{\odot}$, and $E_K = (6.39 \pm 0.70) \times 10^{52} \text{ erg}$, respectively. The quoted errors are statistical only.

4. DISCUSSION

Our photometric and spectroscopic campaign has led to the unambiguous discovery of an SN Ic-BL, SN 2013cq (de Ugarte Postigo et al. 2013), associated with GRB 130427A at $z = 0.34$. GRB 130427A is one of the most energetic bursts ever detected with $E_{\text{iso}} \sim 9.6 \times 10^{53} \text{ erg}$, comparable to that of high-redshift GRBs and much larger than local events. The fact that an SN progenitor model accounts for even very energetic bursts suggests that a common progenitor model, such as the collapsar model, may account for the majority of all long-duration GRBs. To overcome the challenge of providing enough energy to power the GRB, it is likely that the large observed energy is due to beaming (for the strong beaming of GRB 130427A, see Laskar et al. 2013), making the true energy much lower (typically by two orders of magnitude).

Our discovery now suggests that not only core-collapse SNe, but specifically stripped envelope, high-velocity SNe, are almost an inevitable consequence of the deaths of stars that form all GRBs. A common mechanism is therefore at play powering GRBs with very different high-energy properties.

It is worth noting that the comparable peak B-band luminosities of SN 2013cq and SN 1998bw are consistent with the suggestion of Hjorth (2013) that there is an upper envelope to the brightness of GRB-SNe that drops slightly with isotropic luminosity. The origin of such an upper envelope is intriguing, but currently not clear.

As shown in Modjaz et al. (2011), among previous GRB-SN events, the highest oxygen abundance $\log(\text{O/H}) + 12$ at the SN position was less than 8.3. These authors furthermore showed that when the oxygen abundance rises toward a seemingly critical value of 8.5, GRB-SN events tend to locate in dwarf galaxies with $M_{B,\text{host}} > -19.0 \text{ mag}$. Note that the abundance value of 8.5 is a typical one for SNe Ic-BL without observed GRBs, which occur in both luminous and dwarf galaxies. This abundance value is also typical for SNe Ib+Iib, which happen in relatively luminous galaxies with $M_{B,\text{host}} < -18.5 \text{ mag}$ (Modjaz et al. 2011). With an abundance of 8.43 ± 0.07 for the SN position and $M_B = -19.8 \pm 0.2 \text{ mag}$ for the host, GRB 130427A/SN 2013cq is consistent with subclasses of core-collapse SNe such as SNe Ic-BL without observed GRBs and SNe Ib+Iib in the metallicity– $M_{B,\text{host}}$ plane, implying that GRBs do not exclusively explode in low-metallicity dwarf galaxies.

²³ Note that we are using and transforming a bolometric light curve of SN 1998bw that has been constructed using observational data in UBVRIJH filters.

We thank the referee for valuable comments and suggestions. We are grateful to Jens Jessen-Hansen, Tiina Liimets, Dagmara Oszkiewicz, Yeisson Martinez-Osorio, Olesja Smirnova, Jari Kajava, Tuomas Kangas, Emanuel Gafton, Anthony Macchavello, Tore Mansson, and Joachim Wiegert for taking images at the NOT. We are also grateful to Jinyi Yang for carrying out observations at the Xinglong 2.16 m telescope. D.X. thanks Adam S. Trotter for helpful discussions. D.X., J.P.U.F., and B.M.J. acknowledge support from the ERC-StG grant EGGS-278202. A.d.U.P. acknowledges support from the European Commission under the Marie Curie Career Integration Grant program (FP7-PEOPLE-2012-CIG 322307). A.d.U.P., C.T., and J.G. are supported by the Spanish research project AYA2012-39362-C02-02. G.L. is supported by the Swedish Research Council through grant No. 623-2011-7117. Z.C. and P.J. acknowledge support from the Icelandic Research Fund. S.S. acknowledges financial support from the Iniciativa Científica Milenio grant P10-064-F (Millennium Center for Supernova Science), with input from “Fondo de Innovación para la Competitividad, del Ministerio de Economía, Fomento y Turismo de Chile,” and Basal-CATA (PFB-06/2007). L.P.X., T.M.Z., and Y.C.Z. acknowledge the support of the National Science Foundation of China grants 11103036, 11203034, 11178003, and U1231101, respectively. The Dark Cosmology Centre is funded by the Danish National Research Foundation. Based on observations made with the Nordic Optical Telescope, operated by the Nordic Optical Telescope Scientific Association at the Observatorio del Roque de los Muchachos, La Palma, Spain, of the Instituto de Astrofísica de Canarias. Based on observations made with ESO Telescopes at the La Silla Paranal Observatory under program ID 091.C-0934. Based on observations made with the Gran Telescopio Canarias (GTC), at the Spanish Observatorio del Roque de los Muchachos (La Palma). This work made use of data supplied by the UK *Swift* Science Data Centre at the University of Leicester.

REFERENCES

- Aihara, H., Allende Prieto, C., An, D., et al. 2011, *ApJS*, **193**, 29
- Amati, L., Frontera, F., & Guidorzi, C. 2009, *A&A*, **508**, 173
- Arnett, W. D. 1982, *ApJ*, **253**, 785
- Arnouts, S., Cristiani, S., Moscardini, L., et al. 1999, *MNRAS*, **310**, 540
- Asplund, M., Grevesse, N., Grevesse, A. J., et al. 2009, *ARA&A*, **47**, 481
- Beuermann, K., Hessman, F. V., Reinsch, K., et al. 1999, *A&A*, **352**, L26
- Bromberg, O., Nakar, E., & Piran, T. 2011, *ApJ*, **739**, 55
- Bruzual, G., & Charlot, S. 2003, *MNRAS*, **344**, 1000
- Bufano, F., Pian, E., Sollerman, J., et al. 2012, *ApJ*, **753**, 67
- Butler, N. R., Kocevski, D., Bloom, J. S., & Curtis, J. L. 2007, *ApJ*, **671**, 656
- Butler, N. R., Watson, A. M., Kutyrev, A., et al. 2013, GCN Circ., **14483**
- Cano, Z. 2013, *MNRAS*, **434**, 1098
- Cano, Z., Bersier, D., Guidorzi, C., et al. 2011a, *MNRAS*, **413**, 669
- Cano, Z., Bersier, D., Guidorzi, C., et al. 2011b, *ApJ*, **740**, 41
- Della Valle, M., Chincarini, G., Panagia, N., et al. 2006, *Natur*, **444**, 1050
- de Ugarte Postigo, A., Xu, D., Leloudas, G., et al. 2013, *CBET*, **3531**
- Elenin, L., Volnova, A., Savanevych, V., et al. 2013, GCN Circ., **14450**
- Fan, Y. Z., Tam, P. H. T., Zhang, F. W., et al. 2013, *ApJ*, in press (arXiv:1305.1261)
- Fermi-LAT Collaboration. 2013, *ApJS*, submitted (arXiv:1303.2908)
- Fynbo, J. P. U., Watson, D. J., Thöne, C. C., et al. 2006, *Natur*, **444**, 1047
- Galama, T. J., Vreeswijk, P. M., van Paradijs, J., et al. 1998, *Natur*, **395**, 670
- Gal-Yam, A., Fox, D. B., Price, P. A., et al. 2006, *Natur*, **444**, 1053
- Hjorth, J. 2013, *RSPTA*, **371**, 20120275
- Hjorth, J., & Bloom, J. S. 2012, in Gamma-Ray Bursts (Cambridge Astrophysics Series 51), ed. C. Kouveliotou, R. A. M. J. Wijers, & S. Woosley (Cambridge: Cambridge Univ. Press), 169
- Hjorth, J., Sollerman, J., Möller, P., et al. 2003, *Natur*, **423**, 847
- Ilbert, O., Arnouts, S., McCracken, H. J., et al. 2006, *A&A*, **457**, 841
- Jakobsson, P., Hjorth, J., Malesani, D., et al. 2012, *ApJ*, **752**, 62
- Kewley, L. J., & Ellison, S. L. 2008, *ApJ*, **681**, 1183
- Krühler, T., Greiner, J., Schady, P., et al. 2011, *A&A*, **534**, 108
- Laskar, T., Berger, E., Zauderer, B. A., et al. 2013, *ApJ*, submitted (arXiv:1305.2453)
- Levan, A. J., Cenko, S. B., Perley, D. A., & Tanvir, N. R. 2013, GCN Circ., **14455**
- MacFadyen, A. I., & Woosley, S. E. 1999, *ApJ*, **524**, 262
- Maselli, A., Beardmore, A. P., Lien, A. Y., et al. 2013, GCN Circ., **14448**
- McBreen, S., Krühler, T., Rau, A., et al. 2010, *A&A*, **516**, 71
- Modjaz, M., Kewley, L., Bloom, J. S., et al. 2011, *ApJL*, **731**, L4
- Patat, F., Cappellaro, E., Danziger, J., et al. 2001, *ApJ*, **555**, 900
- Perley, D. A., & Cenko, B. 2013, GCN Circ., **14456**
- Pettini, M., & Pagel, B. E. J. 2004, *MNRAS*, **348**, 59
- Pian, E., Mazzali, P. A., Masetti, N., et al. 2006, *Natur*, **442**, 1011
- Piran, T. 2004, *RvMP*, **76**, 1143
- Planck Collaboration. 2013, *A&A*, submitted (arXiv:1303.5076)
- Poznanski, D., Prochaska, J. X., & Bloom, J. S. 2012, *MNRAS*, **426**, 1465
- Schlegel, D. J., Finkbeiner, D. P., & Davis, M. 1998, *ApJ*, **500**, 525
- Sollerman, J., Jaunsen, A. O., Fynbo, J. P. U., et al. 2006, *A&A*, **454**, 503
- Stanek, K. Z., Matheson, T., Garnavich, P. M., et al. 2003, *ApJL*, **591**, L17
- Tam, P. H. T., Tang, Q. W., Hou, S. J., et al. 2013, *ApJL*, **771**, L13
- Tanvir, N. R., Rol, E., Levan, A. J., et al. 2010, *ApJ*, **725**, 625
- von Kienlin, A. 2013, GCN Circ., **14473**
- Wiggins, P. 2013, GCN Circ., **14490**
- Woosley, S. E., & Bloom, J. S. 2006, *ARA&A*, **44**, 507
- Wren, J., Vestrand, W. T., Wozniak, P., et al. 2013, GCN Circ., **14476**
- Zhao, X. H., Mao, J., Wang, J. G., et al. 2013, GCN Circ., **14509**